Available online at www.sciencedirect.com
ScienceDirect
Journal of Volcanology and Geothermal Research 160 (2007) 210–222
Journal of volcanology and geothermal research
www.elsevier.com/locate/jvolgeores

Geometric and kinematic variations along the active Pernicana fault: Implication for the dynamics of Mount Etna NE flank (Italy)

Alessandro Bonforte *, Stefano Branca, Mimmo Palano

Istituto Nazionale di Geofisica e Vulcanologia-Sezione di Catania, Piazza Roma 2, 95123 Catania, Italy

Received 3 February 2006; received in revised form 9 August 2006; accepted 29 August 2006
Available online 20 October 2006

Abstract

Geological and structural analyses and ground deformation measurements performed along the eastern portion of the Pernicana fault system and its splay segments allow the structural setting and the kinematic behaviour of the fault to be defined. In addition, the interrelationship between the deformation style of fault segments and the variations of the volcanic pile thickness along the fault strike are investigated using detailed sedimentary basement data. Brittle deformation dominates the N105° fault segment, where the volcanic pile is more than 200 m thick, with the development of a well-defined fault plane characterised by main left-lateral kinematics. The transtensive deformation of the N105° fault is partitioned eastward at Rocca Campana to a main N120° segment. Here, this segment crosses a culmination of the sedimentary basement close to Vena village where the deformation pattern of the thin volcanic pile, less than 100 m thick, is influenced by the more ductile behaviour of the basement generating local short structures with different orientation and kinematics in the southern block of the fault. On the northern one, short E–W trending faults show left-lateral displacements with a minor reverse component on south-dipping planes. This kinematics is related to the oblique orientation of the N120° segment with respect to the seaward motion of the NE flank of Etna. On the whole, the compressive component of the deformation affecting the N120° segment of the Pernicana fault system generates a positive flower structure.

Keywords: faults; ground deformation; Mt. Etna

1. Introduction

Mount Etna is a basaltic composite strato-volcano, about 3340 m-high, located along the Ionian coast in eastern Sicily (Italy) (Fig. 1).

The volcanic edifice is characterised by a complex geodynamic setting resulting from the combination of regional tectonics and flank instability (Bousquet and Lanzafame, 2004). The eastern flank of the volcano is affected by a continuous ESE seaward sliding due to the interrelationship between gravity instability and magma intrusion (Guest et al., 1984; Borgia et al., 1992; Lo Giudice and Rasà, 1992; McGuire et al., 1996; Montalto et al., 1996; Rust and Neri, 1996; Tibaldi and Groppelli, 2002; Acocella et al., 2003; Bonforte and Puglisi, 2003; Rust et al., 2005; Walter et al., 2005). The northern boundary of the unstable eastern sector of the volcano is formed by the NE-Rift and the Pernicana fault system that are commonly indicated as segments of a near continuous left-lateral shear zone dissecting the NE flank of Etna (Groppelli and Tibaldi, 1999). The kinematics of the Pernicana fault system are also

* Corresponding author. Tel.: +39 0957165809; fax: +39 095435801.
E-mail address: bonforte@ct.ingv.it (A. Bonforte).

0377-0273/$ - see front matter © 2006 Elsevier B.V. All rights reserved.
doi:10.1016/j.jvolgeores.2006.08.009

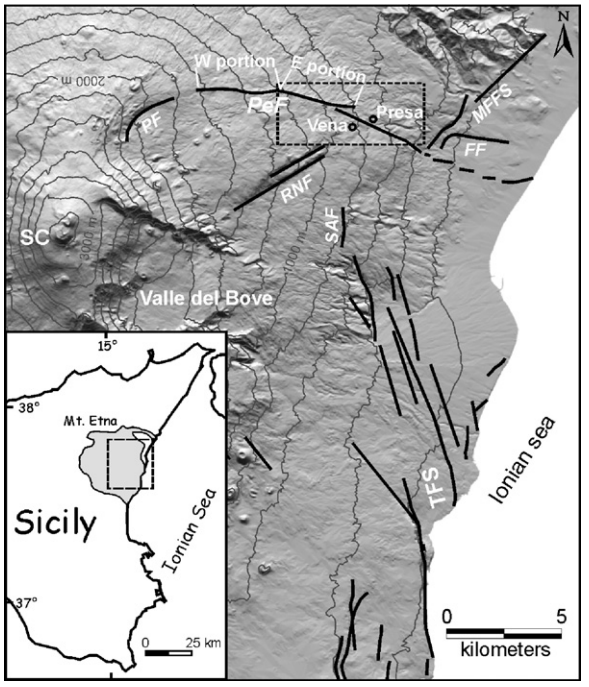

Fig. 1. Structural sketch map of the eastern flank of Etna volcano, SC = Summit Craters. The lower eastern flank is dissected by regional structures related to the Timpe fault system (TFS), NNW-trending, and the Messina-Fiumefreddo fault system (MFFS), NNE-trending (Lentini et al., 1996). Conversely, Provenzana fault (PF), Pernicana fault system (PeF), Fiumefreddo fault (FF), Ripe della Naca faults (RNF) and S. Alfio fault (SAF) are structures generated by the large-scale spreading affecting the eastern flank. The box indicates the study area.

revealed by shallow seismic crises that occur along the western portion of the Pernicana fault, E–W oriented (Fig. 1), with dip–slip displacements coupled with minor left-lateral components (Azzaro, 1997, 2004). Conversely, the eastern portion of the fault, ESE trending, is only affected by aseismic creep with purely left-lateral displacement of about 2 cm/yr, reconstructed over the past 150 yr (Rasà et al., 1996). The eastward propagation of the Pernicana fault was identified for the first time by Azzaro et al. (1998), who evidenced the presence of several splay segments that gradually partition the fault motion close to Vena and Presa villages (Fig. 1). In this area, geodetic data reveal a near-continuous sliding with a stable slip-rate of 2.8 cm/yr (Azzaro et al., 2001). Short N–S oriented reverse faults, less than 100 m-long, link the right-stepping splay segments due to the huge left-lateral motion close to Presa (Acocella and Neri, 2005). During the onset of the 2002–03 flank eruption, huge ground fracturing involved the entire north-eastern flank allowing identifying the development of the splay segments down to the Ionian coast (Neri et al., 2004), as hypothesised from geodetic data spanning from 1997 to 2001 by Bonforte and Puglisi (2006). In addition to the transtensive tectonics of the Pernicana fault, a compressive strain was measured, for the first time, by GPS data that showed a roughly N–S contraction in correspondence of the July 3rd 1994 earthquake (Puglisi et al., 2001). Furthermore, an inverse component movement of the fault has also been modelled from geodetic data acquired from a local GPS network (hereafter RCN network), although not supported by geological evidence (Azzaro et al., 2001). Finally, activation of the fault with reverse kinematics has been detected from GPS measurements by Palano et al. (in press) on the RCN network.

In this paper, we present the results of a multidisciplinary study based on geological-structural investigations and geodetic measurements integrated with sedimentary basement data, in order to clarify the complex kinematics affecting both the eastern portion of the Pernicana fault and its splay segments close to Vena and Presa villages.

2. Geological and structural data

The oldest volcanic rocks are deep-weathered lava flows and a scoria cone resting on the Early-Middle Pleistocene marly-clays (Fig. 2), which are related to the early phase of the alkaline-Na eruptive activity of Etna (Timpe phase of Branca et al., 2004a). These products are partially covered by an alluvial deposit that grades upward into a debris flow deposit. Lava flows and pyroclastic deposits related to the Ellittico volcano activity consist of isolated outcrops resting both on sedimentary basement and interlayered with the top of the debris flow deposit. In particular, the pyroclastic deposits are made up of an alternation of scoriaceous lapilli and ash layers about 2.8 m thick (Andronico et al., 2001), cropping out only at Contrada Ragaglia locality (Fig. 2). The final phase of the Ellittico volcano activity is represented by a pumice fall deposit related to plinian eruptions occurring about 15 ka ago (Coltelli et al., 2000) that discontinuously covered the previous products. The lava flows of the effusive activity of the last 15 ka (Mongibello volcano, Branca et al., 2004a) consist of several superimposed lava flow fields that are widely distributed in the investigated area (Fig. 2). The Mongibello lava succession is subdivided into temporal intervals according to the guidelines defined during the drawing up of the new geological map of Etna (Branca et al., 2004b), in which Holocene marker beds were used to better constrain the age of the lava flows. In particular,

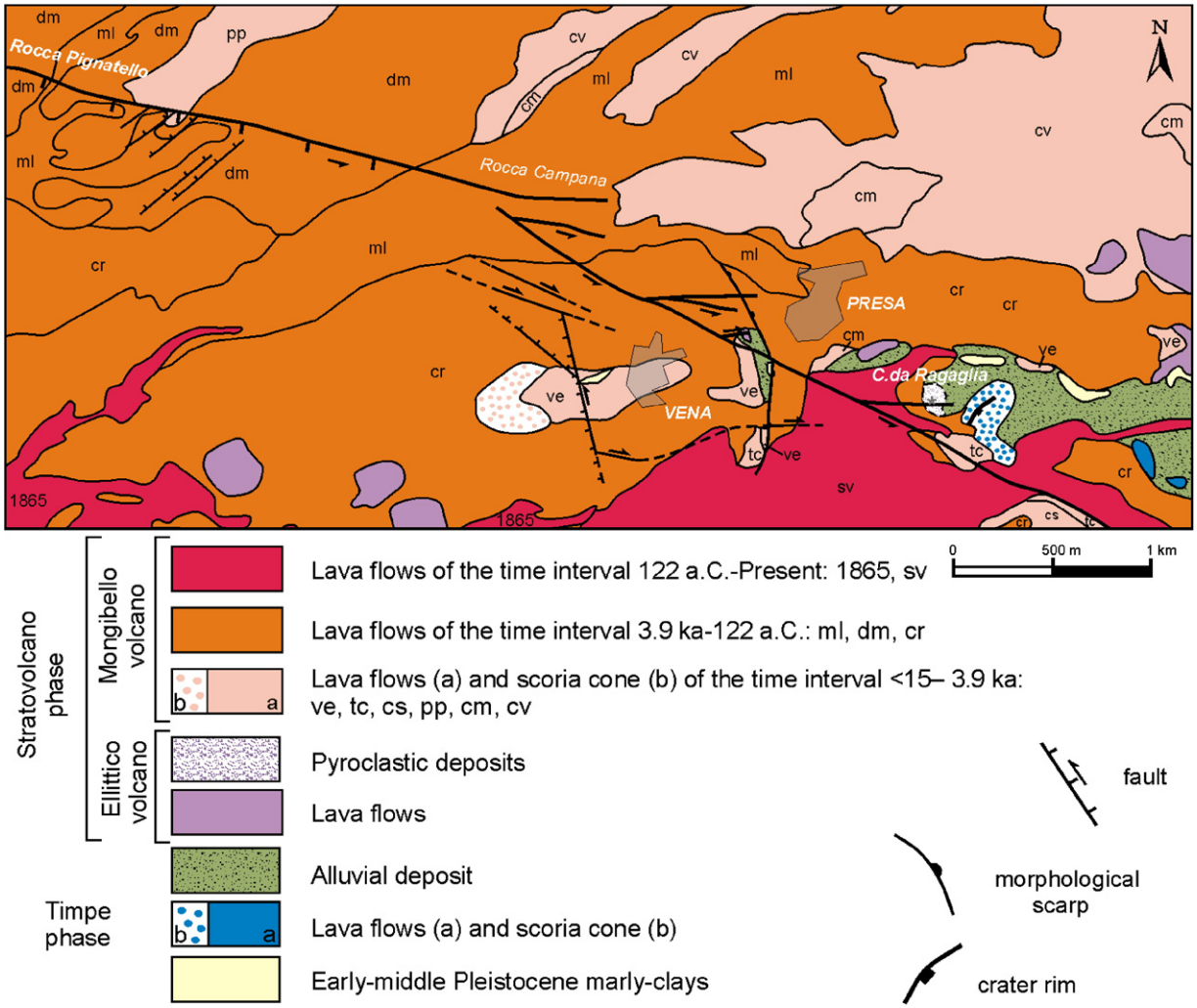

Fig. 2. Geological map of the investigated area. The stratigraphic frame is according to the new Etna volcano stratigraphy proposed by Branca et al. (2004a). Letters indicate distinct lava flow fields of the last 15 ka.

the marker beds are represented by two pyroclastic fallout deposits generated by sub-plinian eruptions dated 3930±60 yr BP (FS tephra layer of Coltelli et al., 2000) and by a plinian eruption in 122 B.C. (FG tephra layer of Coltelli et al., 2000). The oldest Mongibello lava flow in the study area, dated about 10.9 ka (Andronico et al., 2001), rests on the sedimentary basement and is generated by a scoria cone located west of Vena (ve in Fig. 2). The lava flows of the last 3.9 ka activity consist of wide lava flow fields forming the main portion of the study area that have veiled the original morphology of the pre-volcanic basement.

The investigated area is dissected by two principal segments of the Pernicana fault (Fig. 3): the first shows a roughly N105° orientation dissecting the area from Rocca Pignatello to Rocca Campana; here the fault rotates to N90° and terminates without morphological evidences. The second propagates downhill from Rocca Campana with a roughly N120° orientation. Both segments show a clear left-lateral strike–slip displacement. A series of short structures intersect the two segments of the Pernicana fault. These secondary structures show variable orientation and are developed both on the southern and northern blocks (Fig. 3):

(1) at Rocca Pignatello area, an extensional fracture field, N40° oriented, locally creates sag ponds and graben-like features on the southern block;
(2) between Rocca Campana and Presa, another series of short splay segments developed along the northern block of the N120° fault are recognized. These short splays are characterised by left and

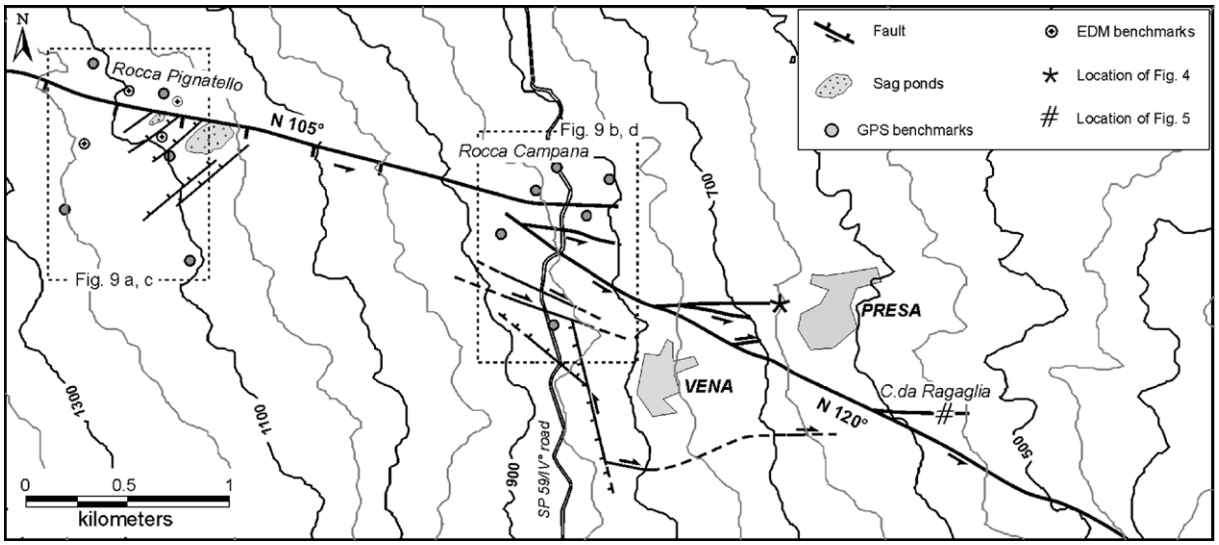

Fig. 3. Structural sketch map and location of the geodetic networks. The two boxes show the areas reported in Fig. 9.

right-lateral displacements with a minor reverse component on south-dipping fault planes, E–W oriented, as evidenced by the reverse faults dissecting some concrete walls (Fig. 4);

(3) in the southern block of the N120° fault, near Vena, complex short structures with orientation ranging from N90° to N170° are developed. These structures, showing both left and right-lateral movement with minor normal dip–slip component, were evidenced for the first time during the huge surface fracturing related to the onset of 2002–03 flank eruption (Neri et al., 2004);

(4) at Contrada Ragaglia locality (520 m a.s.l.), transpressive structures affect the Ellittico pyroclastic deposits on the northern block of the N120° fault. In this area a set of reverse faults, oriented N90°–100° and having leading-imbricate fan geometry, offset the lapilli and ash layers with a south-dipping high-angle fault plane ranging from 40° to 75° (Fig. 5a). On the whole, the Ellittico pyroclastic deposits are deformed in a fault-bend fold style linked to the presence of ramp-flat structures (Figs. 5b and 6).

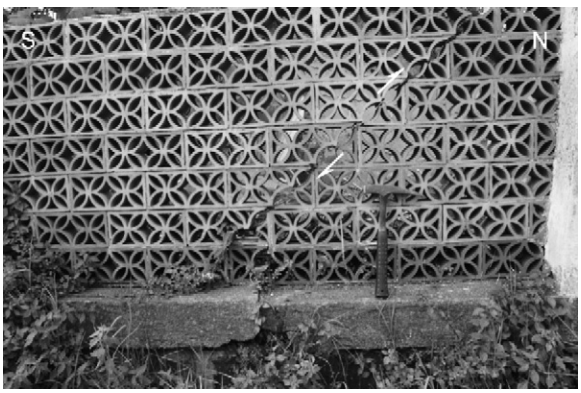

Fig. 4. Photograph of a reverse fault, south-dipping, dissecting a concrete wall close to Presa village. For the location see Fig. 3.

3. Sedimentary basement data

Data from Branca and Ferrara (2001) and from unpublished subsurface data for ground water investigation (Regione Siciliana-Assessorato, 1994), allowed us to highlight the complex morphological setting of the sedimentary basement below the investigated area. The subsurface data consist of geoelectric soundings that were calibrated through several coring boreholes reaching the sedimentary basement (Fig. 7a). The large number of geoelectric soundings allowed the detailed reconstruction of the conductive substrate trend, corresponding to the top of the sedimentary basement, with a high resolution quality. In particular, the confidence value of the depth of the volcanic pile-sedimentary basement transition, obtained through the geoelectric measurements, is generally less than 20%.

Early-Middle Pleistocene marly-clays outcrop discontinuously from about 200 up to 770 m a.s.l. close to Vena (Fig. 2) indicating the presence of a sedimentary ridge oriented E–W (Fig. 7a). Previously, Groppelli and Tibaldi (1999) interpreted the presence of the Pleistocene sediment outcrops as the expression of a bulge

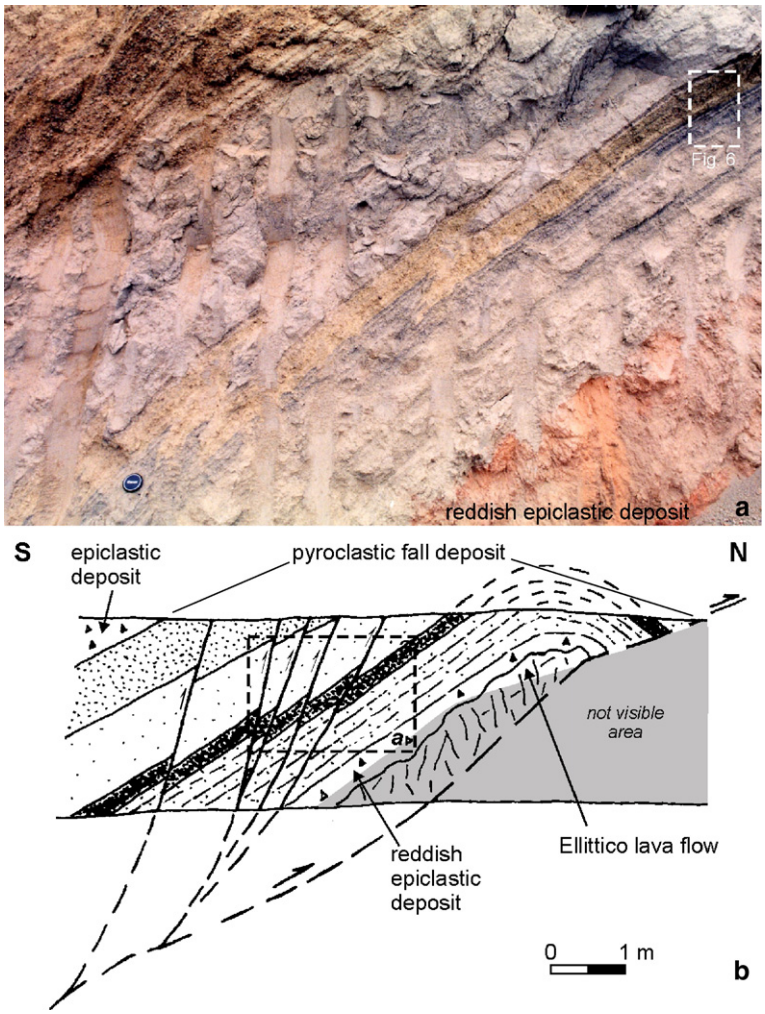

Fig. 5. a) Photograph taken along a wall of a terrace-cultivation at Contrada Ragaglia locality showing the reverse faults, south-dipping, that dissect the pyroclastic lapilli and ash layers of the Ellittico volcano resting on a reddish epiclastic deposits. The lens cover, 6.2 cm long, provides a scale. The white box indicates the location of Fig. 6; b) schematic sketch of the Contrada Ragaglia outcrop illustrating the fault-bend fold structure affecting the Ellittico products. The wall of the terrace-cultivation is about 8.5 m long and 2.5 m high. In grey is the area of the terrace-cultivation cover by detritus. The box shows the location of the photograph (a).

zone of Holocene deformation related to the Pernicana fault system. Conversely, the reconstruction of the whole sedimentary basement below the NE flank of Etna by Branca and Ferrara (2001) indicated that this E–W trending sedimentary ridge is the buried southern flank of the Alcantara river paleovalley formed at least during the past 100 ka (Branca, 2003).

The portion of the sedimentary ridge in the study area generally slopes eastwards from about 800 to 200 m a.s.l., showing a local hill-shaped culmination located in correspondence of Vena (Fig. 7a). This culmination reaches an elevation of about 770 m and is characterized by very steep slopes on the northern and eastern sides. Conversely, it slopes gently westward, interrupting the general slope-trend of the ridge. This morphological setting is marked by a narrow and deep drainage gully trending from NW, in its upper part, to NE in the lower one (Fig. 7a).

The volcanic pile thickness was calculated by subtracting the sedimentary topography from a photogrammetric DEM, (accuracy of about 10 m), used as source for the topographic data. The resulting thickness ranges from 0 to about 500 m (Fig. 7b). The sedimentary basement outcrops discontinuously at the hill-shaped culmination and along its eastern slope where the volcanic cover is generally thin (up to a maximum of about 100 m). Conversely, on the western side of the hill-shaped culmination, the thickness

Fig. 6. Detail of Fig. 5a, highlighting the reverse structure with fault-bend fold style of the Ellittico lapilli layers at cm-sized scale that clearly evidences the presence of ramp-flat structures.

dramatically increases reaching a maximum of almost 500 m along the axis of the drainage gully.

4. Geodetic data

Two local geodetic networks were installed by "Istituto Internazionale di Vulcanologia" in April 1997 across the eastern portion of the Pernicana fault, on Rocca Pignatello and Rocca Campana areas (Azzaro et al., 2001; Palano et al., in press) (Fig. 3). GPS technique was adopted to survey the RCN network, while EDM technique was adopted to measure the Rocca Pignatello one (RPN network). The two networks are relatively small, covering an area in the order of 1 km^2 and consisting respectively of 6 and 4 benchmarks. The first measurements of the networks were carried out in early 1997; since then, the networks have been surveyed at least three times per year in order to adequately detected pattern and rate variations of ground deformation. From July 2002, 5 new benchmarks were installed at RPN area and the GPS technique has been adopted to survey them, so in September 2002 the last EDM survey on the old RPN network was carried out.

In order to define the evolution of the ground deformation pattern in the investigated area, the geodetic data collected at different times by EDM or GPS surveys must be comparable. The two adopted surveying techniques produce two different types of information.

The EDM measurements were reduced to ground level (nails) by using appropriate surveying strategies, for instance by always carrying out the measurements at the same instrumental height (Azzaro et al., 2001), and the distances are also corrected by using meteorological data simultaneously acquired during the distance measurements at both ends of the measured baseline. Finally, we directly compared the corrected distance measurements of different surveys in order to obtain the length variations for each baseline.

In the case of GPS, each network could be adjusted by using the same local reference frame among surveys carried out at different times. Due to the small extension of the networks, the tilt of biases eventually introduced by differences in the satellites ephemerides systems is negligible, so the minimal constrain approach using one of the network benchmarks as a fixed point ensures the stability of the reference frame during different surveys. For the surveys considered in this paper, benchmarks PER5 and RPN2 were assumed as fixed points for the RCN and RPN networks respectively. The final solution consists in a set of benchmark coordinates for each survey.

The results of the geodetic surveys are reported in terms of displacement vectors and strain parameters and provide fundamental information to correctly interpret the kinematics of the fault (Fig. 8). Fairly uniform displacement vectors characterize the southern block of the N105° fault at RPN area, clearly related to a left-lateral kinematics; conversely, the more complex structural framework of RCN area produces a more complicated ground deformation field. Here, the deformation is partitioned between the N105° and the N120° faults. The smaller displacements affecting the benchmark PER3 with respect to those affecting benchmarks PER1 and PER2 (Fig. 8a) clearly indicates that the N120° fault accommodates most of the displacement of the N105° fault; geodetic data collected from 1997 to 2001 at lower altitude, confirms that this last structure allows the deformation to propagate down to the coast (Bonforte and Puglisi, 2006). By statistical analyses of the displacement vectors performed for the entire available GPS dataset in Palano et al. (in press), the most frequent direction of movement (24%) measured at benchmark PER2 is N115° indicating the left-lateral kinematics of the N120° fault. This direction

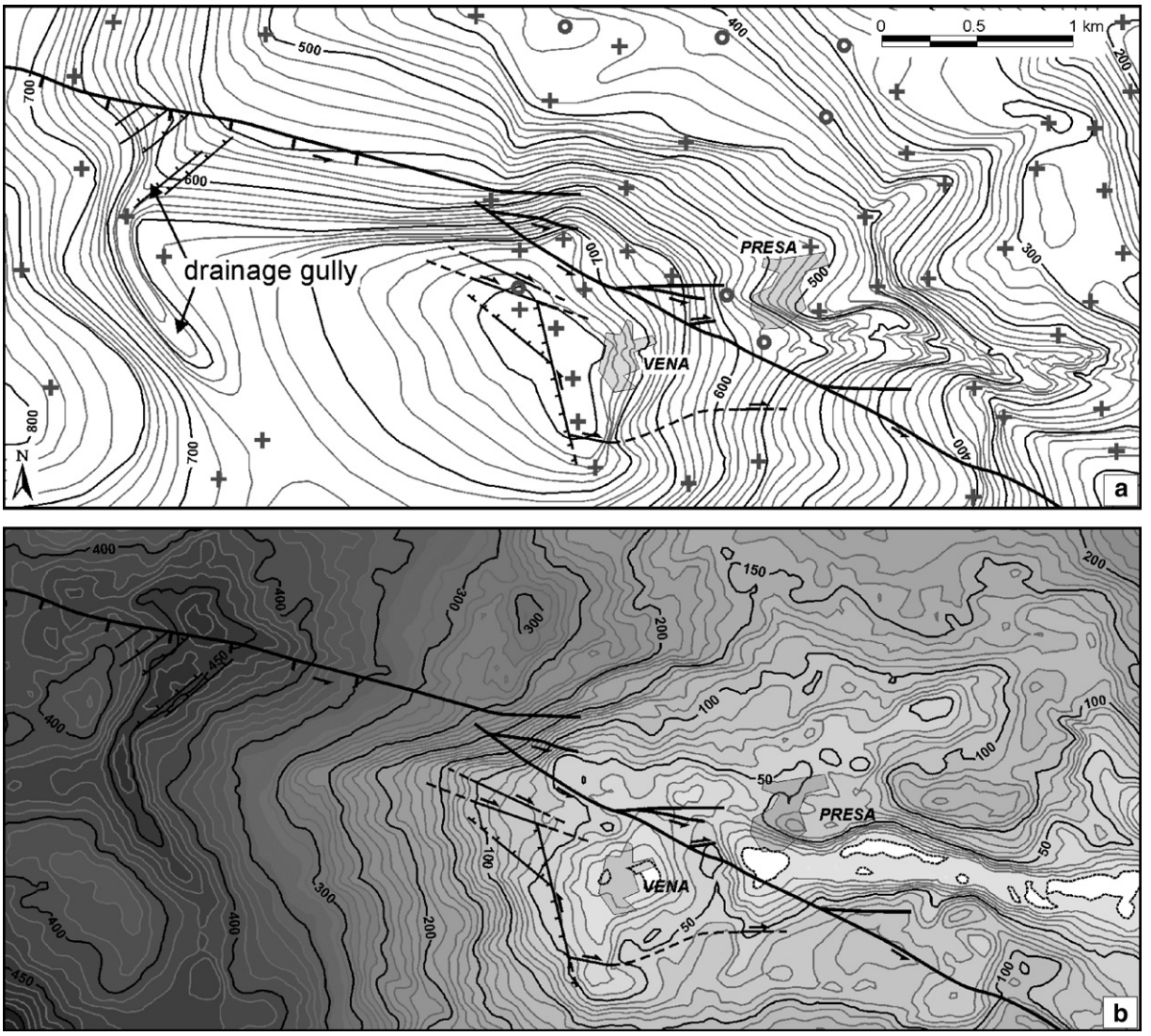

Fig. 7. Topography of the sedimentary basement (a), the black circles are the boreholes and the black crosses are the geoelectric soundings; thickness of volcanic pile (b). The contour interval is 10 m.

of movement shows a component towards the N120° fault, evidencing a second-order reverse motion on this fault.

Concerning the slip-rate values, until the 2002–03 flank eruption onset, at RCN network, an averaged slip-rate of about 1.1 cm/yr for the N105° (measured at PER3 benchmark) and about 2.8 cm/yr for the N120° fault (measured at PER1 and PER2 benchmarks) can be inferred (Palano et al., in press). In this time interval, only a small increase in the slip rate (2.6 cm/yr and 6.5 cm/yr respectively for the N105° fault and the N120° fault respectively) is clearly related to the 2001 flank eruption. High slip-rate values are observed during the first days of the 2002–03 flank eruption. In the months following the eruption, the slip-rate slowly declined until showing values similar to those observed before the eruption onset, with no increase associated with the 2004–05 flank eruption. In the last three surveys (since April 2005) of the time series, a new increase of the slip-rate was recorded. The same pattern has been observed at the RPN network too.

In order to give details of the strain distribution above the investigated area, the networks have been divided into triangles, as close as possible to equilateral, lying across the N105° and the N120° faults. Due to the different time coverage for GPS and EDM techniques at Rocca Pignatello area (from

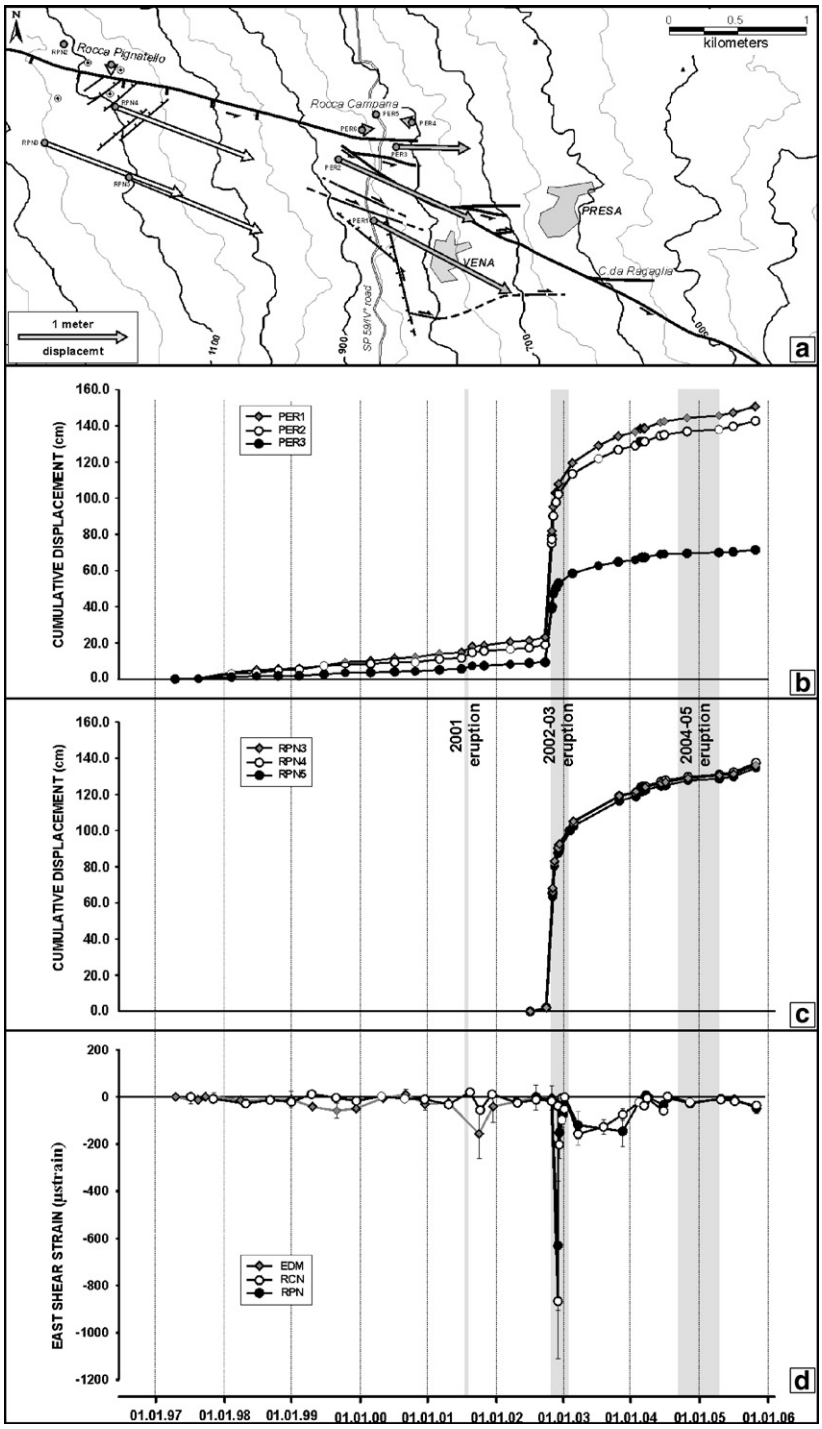

Fig. 8. Cumulative horizontal displacements for the two GPS networks: from April 1997 to November 2005 for the RCN network (displacements with respect to PER5), and from July 2002 to November 2005 for RPN network (displacements with respect to RPN2) (a); time evolution of the displacements of some selected benchmarks of the RCN network (b); time evolution of the displacements of some selected benchmarks of the RPN network (c); time evolution of east shear strain pattern (strain is assumed to be positive for right-lateral shear) (d). Modified from Palano et al. (in press).

January 1997 until July 2002 for EDM and from July 2002 until November 2005 for GPS data) the strain analysis was performed by also splitting the RCN GPS data in two different time intervals. Then, the strain tensor for each triangle was computed by using a least squares algorithm based on the approach suggested by Livieratos (1980), which uses the strain of each baseline as input data. The computation was performed by considering the strain calculated on the ellipsoid distance component of each baseline. The strain field was assumed as irrotational, homogeneous and infinitesimal. As for the displacement vectors, the RPN network shows a uniform strain for different triangles both from EDM (Fig. 9a) and GPS data (Fig. 9c). At RCN network, a clockwise rotation of the strain tensor is visible moving from north to south, gradually changing from NW–SE extension with NE–SW contraction for the triangle that involves only the N105° fault (PER3–PER4–PER5 in Fig. 9b), to N–S extension with E–W contraction for the triangle involving only the N120° fault (PER1–PER2–PER3 in Fig. 9b). Also the effect of the 2002–03 flank eruption, which produced an exceptional slip along the fault, is visible from the strain ellipses from the 2002–2005 interval that evidence an increased deviatoric strain, mainly on the main fault (Fig. 9d).

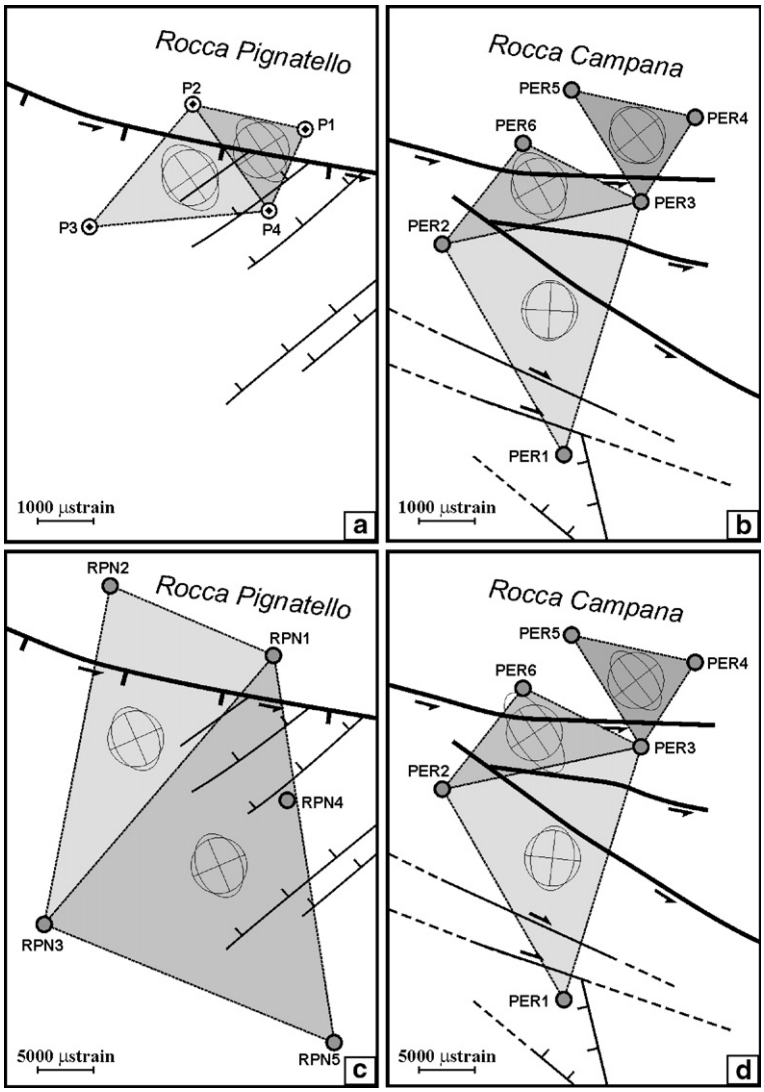

Fig. 9. Strain ellipses for each geodetic network: a, b) from January 1997 until July 2002 and c, d) from July 2002 until November 2005. The measured contraction is in the order of 150 μstrain for the 1997–2002 period, increasing by about one order of magnitude during the 2002–2005 interval due to the effect of the 2002–03 flank eruption.

5. Discussion

Geological and geodetic investigations are performed along the eastern portion of the Pernicana fault, representing the northern boundary of the eastern unstable flank of the volcano, in order to define its complex structural setting and kinematics behaviour. In the investigated area, the Pernicana fault, trending N105°, terminates without morphological evidences at Rocca Campana locality where it branches forming a main segment, trending N120°. Both segments show a main left-lateral strike–slip displacement. All geological and geodetic analyses are, furthermore, integrated and compared with detailed sedimentary basement data, in order to define the possible interrelationship between the kinematics behaviour of the Pernicana fault segments and the variations of the volcanic pile thickness. In fact, the Pernicana fault system is located along an almost buried culmination of the sedimentary basement, E–W oriented, that plays a key role in the complex structural setting of the easternmost portion of the fault.

The development of sector spreading at volcanoes is controlled by the dip and slope of the substrata (Wooler et al., 2004). In particular, the dip of substrata strongly conditions the spreading style and direction with the formation of strike–slip fault systems whose geometry and extent depend both on cone morphology (Merle and Borgia, 1996; van Wyk de Vries et al., 2003) and the presence of substrata inhomogeneities (Bailey, 1998). Concerning the Etna case, its sedimentary basement suffered a long-term asymmetric updoming that resulted in a inhomogeneous morphological setting (Di Stefano and Branca, 2002). In particular, the high eastward gradient slope of the basement below the NE flank of the volcano controls the geometry and the extent of the Pernicana fault system as demonstrated by Wooler et al. (2004) for dipping substrata.

Along the fault strike different rheological behaviours were already inferred by Groppelli and Tibaldi (1999) owing to the thickness variation of the volcanic pile. By analysing the position of the fault with respect to the new detailed substratum data here presented, it is evident how the abrupt decrease in the volcanic cover thickness conditions the structural setting along the southern block of the two fault segments.

In particular, along the N105° fault segment the thickness of the volcanic pile ranges from about 200 m to about 400 m. For this reason, from Rocca Pignatello to Rocca Campana area, the brittle deformation dominates with the development of a unique and well defined fault plane characterised by a uniform strain pattern as measured at RPN network. Here, the presence of a buried drainage gully produces a volcanic wedge (NE–SW oriented) with deeper roots inside the sedimentary basement, well delimited on the surface by a small extensional fracture field, probably due to major rigidity of this wedge (more than 450 m thick) with respect to the surrounding rocks. Conversely, from Rocca Campana, the main N120° fault segment crosses the prominent culmination of the marly-clay basement at Vena. Here, the brittle deformation of the very thin volcanic pile (from 0 to 100 m) is influenced by the plastic behaviour of the underlying basement, accommodating the deformation along the southern block with the development of local short structures with different orientation and kinematics, which border the area of minor thickness (Fig. 7b).

Furthermore, geological and structural data reveal for the first time a reverse component of displacement along E–W oriented fault planes on the northern block of the N125°–115° segment. In fact, reverse faults with south-dipping planes dissect the Ellittico pyroclastic deposits forming a series of fault-bend folds due to the N–S compressive component that are well-exposed at Contrada Ragaglia area (Fig. 5). The geodetic data confirm a different strain affecting the northern block of the N120° fault. In fact, the contraction axis progressively rotates from E–W for the triangle PER1–PER2–PER3 (lying across the N120° fault) to NE–SW for the triangle PER3–PER4–PER5 (lying across the N105° fault), according to the different azimuth of the faults (Fig 9b and d). The strain ellipses computed for the PER3–PER4–PER5 triangle predict a maximum shear strain along a N90°–100° direction, according to the change in the azimuth of the N105° fault that assumes an almost E–W orientation at Rocca Campana. Conversely, the calculated strain ellipses at Rocca Pignatello predict a maximum shear strain along a N110–120° implying an extension component along the actual N105° trending fault.

This abrupt change in the kinematics behaviour of the left-lateral shear zone that dissects the north-eastern flank of Etna seems to be closely related to the orientation of the N120° fault with respect to the general ESE motion of the entire seaward-sliding NE flank of the volcano (Bonforte and Puglisi, 2006). In fact, the displacement vectors of the southern benchmarks of both networks show an azimuth of N115°. This means that at Rocca Pignatello (e.g. RPN4) the sliding block moves away from the fault trace (here N105° trending) revealing an extension component; conversely, at Rocca Campana the azimuth of the

displacement vectors of the southern benchmarks (e.g. PER2) intersect the N120° direction of the main fault plane producing a constant reverse component coupled to the main left-lateral movement (Fig 9a). In this area, the kinematics change from purely left-lateral strike–slip to a transpressive left-lateral movement forming a positive flower structure (Fig. 10).

On the whole, the geodetic data collected since 1997 have outlined that the Pernicana fault is characterised by a fairly stable and constant slip rate, in the order of about 2.8 cm/yr, related to the dynamics of the eastern flank of the volcano that is affected by a continuous gravitational sliding motion toward the sea (Bonforte and Puglisi, 2003). Furthermore, the kinematics of the fault is sometimes perturbed by additional stress related to dyke intrusions in the upper part of the volcano as indicated by an abrupt increase in the slip rate in concomitance of some eruptive events, evidencing a complex relationship between flank slip and volcanic activity. In particular, the dynamics of the Pernicana fault remained stable during the shallow intrusions feeding the 2004–05 eruption (Burton et al., 2005) and only a minor acceleration was observed in occasion of the 2001 flank eruption that was fed by a deep intrusion located on the upper southern flank of the volcano (Musumeci et al., 2004). Conversely, we observed a dramatic acceleration of the slip rate when the magma intrusion involved the NE-Rift during the 2002–03 flank eruption onset. In fact, this structure is directly connected to the Pernicana fault system that allowed the ground deformation induced by the intrusion to propagate eastward showing a progressive decay of the slip rate in time.

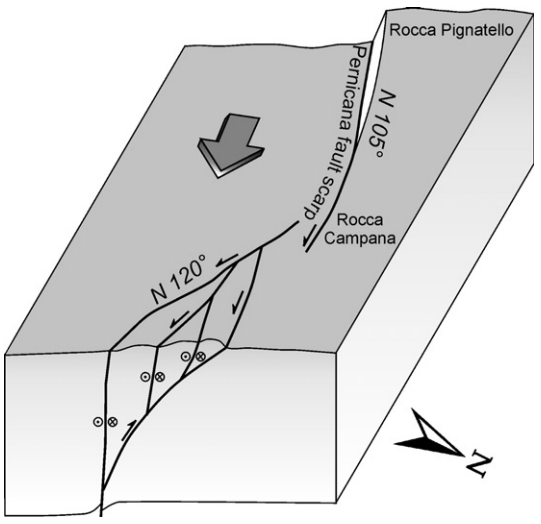

Fig. 10. Interpretative block diagram showing the kinematics behaviour of the Pernicana fault system from Rocca Pignatello to Vena and Presa villages according to the geological-structural and geodetic data. The arrow indicates the mean motion direction of the seaward sliding north-eastern flank.

6. Concluding remarks

Multidisciplinary studies performed along the eastern portion of the Pernicana fault system allow us to better define the complex structural setting and the kinematic behaviour of the most active deformation system on Etna volcano and to delineate its relationship with the sedimentary basement morphology. Taking into account the geological and geodetic data we can synthesize the main results in the following point:

(1) the Pernicana fault system is located along an almost buried culmination of the sedimentary basement, E–W oriented, where the variation of the volcanic pile thickness along the fault strike controls its structural setting;
(2) along the N105° fault segment the brittle deformation dominates with the development of a unique and well defined fault plane characterised by a uniform strain pattern with a main left-lateral kinematics. Effects of volcanic thickness variations are here revealed only by a small extensional fracture field, that follows the orientation of a buried drainage gully at Rocca Pignatello;
(3) the N105° fault segment terminates without morphological evidence at Rocca Campana locality, where the deformation is transferred eastward to a main segment N120° oriented;
(4) the N120° oriented segment crosses a prominent culmination of the sedimentary basement in correspondence of Vena village. Here, the very thin volcanic cover, accommodates the plastic deformation of the sedimentary basement with the development of several short fault segments, different in orientation and kinematics;
(5) the main direction of the sliding motion of the eastern flank of the volcano, revealed by GPS data both at RPN and RCN networks, intersects the N120° segment strike, thus producing a constant reverse component coupled to the main left-lateral movement generating a positive flower structure;
(6) the long-term behaviour of the slip rate of the Pernicana fault system measured from 1997 to 2006 evidences a constant and continuous motion related to the gravitational spreading of eastern flank that is occasionally accelerated by volcanic activity.

In terms of flank spreading, the form and extent of the unstable eastern flank of Etna edifice is strictly connected to the inhomogeneous morphological setting of the sedimentary basement. In particular, in this paper we evidenced that the presence of a well-developed eastward-dipping basement culmination strongly controls the geometry and the kinematics of the northern boundary of the spreading sector of the volcano. In the light of this consideration, detailed knowledge of the morphology of Etna's basement is a key to better understand the complex kinematic behaviour of the volcano's entire eastern flank.

Acknowledgments

We are grateful to G. Puglisi, R. Azzaro and M. Coltelli for the revision of an earlier version of the manuscript, and to P. Guarnieri for the helpful suggestions concerning the structural data. The reviewers V. Acocella and A. Duncan are acknowledged for their useful comments that improved the manuscript.

References

Acocella, V., Neri, M., 2005. Structural features of an active strike–slip fault on the sliding flank of Mt. Etna (Italy). J. Struct. Geol. 27, 343–355.

Acocella, V., Behncke, B., Neri, M., D'Amico, S., 2003. Link between major flank slip and 2002–2003 eruption at Mt. Etna (Italy). Geophys. Res. Lett. 30 (24), 2286. doi:10.1029/2003GL018642.

Andronico, D., Branca, S., Del Carlo, P., 2001. The 18.7 ka phreatomagmatic flank eruption on Etna (Italy): relationship between eruptive activity and sedimentary basement setting. Terra Nova 13 (4), 235–240.

Azzaro, R., 1997. Seismicity and active tectonics along the Pernicana fault Mt. Etna (Italy). Acta Vulcanol. 9, 7–14.

Azzaro, R., 2004. Seismicity and active tectonic in the Etna region: constrain for seismotectonic model. In: Bonaccorso, A., Calvari, S., Coltelli, M., Del Negro, C., Falsaperla, S. (Eds.), Mt. Etna Volcano Laboratory. Am. Geoph. Union (Geophysical monograph series), vol. 143, pp. 205–220.

Azzaro, R., Branca, S., Giammanco, S., Gurrieri, S., Rasà, R., Valenza, M., 1998. New evidence for the form and extent of the Pernicana fault system (Mt. Etna) from structural and soil–gas surveying. J. Volcanol. Geotherm. Res. 84, 143–152.

Azzaro, R., Mattia, M., Puglisi, G., 2001. Fault creep and kinematics of the eastern segment of the Pernicana Fault (Mt. Etna, Italy) derived from geodetic observation and their tectonic significance. Tectonophysics 333, 401–415.

Bailey, R.C., 1998. Thresholds for gravitationally induced thrusting by elevated topography over a ductile crust. GSA Abstracts with Programs, vol. 30, no. 7, p. 297.

Bonforte, A., Puglisi, G., 2003. Magma uprising and flank dynamics on Mount Etna volcano, studied using GPS data (1994–1995). J. Geophys. Res. 108 (B3), 2153.

Bonforte, A., Puglisi, G., 2006. Dynamics of the eastern flank of Mt. Etna volcano (Italy) investigated by a dense GPS network. J. Volcanol. Geotherm. Res. 153, 357–369.

Borgia, A., Ferrari, L., Pasquarè, G., 1992. Importance of gravitational spreading in the tectonic and volcanic evolution of Mount Etna. Nature 357, 231–235.

Bousquet, J.C., Lanzafame, G., 2004. The tectonics and geodynamics of Mt. Etna: synthesis and interpretation of geological and geophysical data. In: Bonaccorso, A., Calvari, S., Coltelli, M., Del Negro, C., Falsaperla, S. (Eds.), Mt. Etna Volcano Laboratory. Am. Geoph. Union (Geophysical monograph series), vol. 143, pp. 29–48.

Branca, S., 2003. Geological and geomorphologic evolution of the Etna volcano NE flank and relationships between lava flow invasions and erosional processes in the Alcantara Valley (Italy). Geomorphology 53, 247–261.

Branca, S., Ferrara, V., 2001. An example of river pattern evolution produced during the lateral growth of a central polygenic volcano: the case of the Alcantara river system, Mt Etna (Italy). Catena 45 (2), 85–102.

Branca, S., Coltelli, M., Groppelli, G., 2004a. Geological evolution of Etna volcano. In: Bonaccorso, A., Calvari, S., Coltelli, M., Del Negro, C., Falsaperla, S. (Eds.), Mt. Etna Volcano Laboratory. Am. Geoph. Union (Geophysical monograph series), vol. 143, pp. 49–63.

Branca, S., Coltelli, M., Del Carlo, P., Groppelli, G., Norini, G., Pasquaré, G., 2004b. Stratigraphical approaches and tools in the geological mapping of Mt. Etna Volcano. In: Pasquarè, G., Venturini, C. (Eds.), Mapping Geology in Italy. APAT-SELCA, Roma, pp. 145–156.

Burton, M.R., Neri, M., Andronico, D., Branca, S., Caltabiano, T., Calvari, S., Corsaro, R.A., Del Carlo, P., Lanzafame, G., Lodato, L., Miraglia, L., Salerno, G., Spampanato, L., 2005. Etna 2004–2005: an archetype for geodynamically-controlled effusive eruptions. Geophys. Res. Lett. 32, L09303. doi:10.1029/2005GL022527.

Coltelli, M., Del Carlo, P., Vezzoli, L., 2000. Stratigraphic constrains for explosive activity in the last 100 ka at Etna volcano. Italy. Int. J. Earth Sci. 89, 665–677.

Di Stefano, A., Branca, S., 2002. Long-term uplift rate of the Etna volcano basement (Southern Italy) from biochronological data of the Pleistocene sediments. Terra Nova 14 (1), 61–68.

Groppelli, G., Tibaldi, A., 1999. Control of rock rheology on deformation style and slip-rate along the active Pernicana Fault, Mt. Etna, Italy. Tectonophysics 305, 521–537.

Guest, L.E., Chester, D.R., Ducan, A.M., 1984. The Valle del Bove, Mount Etna: its origin and relation to the stratigraphy and structure of the volcano. J. Volcanol. Geotherm. Res. 21, 1–23.

Lentini, F., Carbone, S., Catalano, S., Grasso, M., 1996. Elementi per la ricostruzione del quadro strutturale della Sicilia orientale. Mem. Soc. Geol. Ital. 51, 179–195.

Livieratos, E., 1980. Crustal strain using geodetic methods. Geōd. Tetr. 3, 191–211.

Lo Giudice, E., Rasà, R., 1992. Very shallow earthquakes and brittle deformation in active volcanic areas: the Etnean region as an example. Tectonophysics 202, 257–268.

McGuire, W.J., Moss, J.L., Saunders, S.J., Stewart, I.S., 1996. Dyke-induced rifting and edifice instability at Mount Etna. In: Gravestock, P.J., McGuire, W.J. (Eds.), Etna: 15 Years On. ODA/Cheltenham and Gloucester College of Higher Education, pp. 20–24.

Merle, O., Borgia, A., 1996. Scaled experiments of volcano spreading. J. Geophys. Res. 101, 13,805–13,817.

Montalto, A., Vinciguerra, S., Menza, S., Patanè, G., 1996. Recent seismicity of Mount Etna: implication for flank instability. In: McGuire, W.J., Jones, A.P., Neuberg, J. (Eds.), Volcano Instability on the Earth and other Planets. Geol. Soc. London, Spec. Pub., vol. 110, pp. 169–177.

Musumeci, C., Cocina, O., De Gori, P., Patanè, D., 2004. Seismological evidences of stress induced by dike injection during the 2001 Mt. Etna eruption. Geophys. Res. Lett. 31, L07617. doi:10.1029/2003GL019367.

Neri, M., Acocella, V., Behncke, B., 2004. The role of the Pernicana fault system in the spreading of Mount Etna (Italy) during the 2002–2003 eruption. Bull. Volcanol. 66, 417–430.

Palano, M., Aloisi, M., Amore, M., Bonforte, A., Calvagna, F., Cantarero, M., Consoli, O., Consoli, S., Guglielmino, F., Mattia, M., Puglisi, B., Puglisi, G., in press. Kinematic and strain analyses of the eastern segment of the Pernicana fault (Mt. Etna, Italy) derived from geodetic techniques (1997–2005). Annals of Geophysics.

Puglisi, G., Bonforte, A., Maugeri, S.R., 2001. Ground deformation patterns on Mt. Etna, 1992 to 1994, inferred from GPS data. Bull. Volcanol. 62, 371–384.

Rasà, R., Azzaro, R., Leonardi, O., 1996. Aseismic creep on faults and flank instability at Mount Etna volcano, Sicily. In: McGuire, W.J., Jones, A.P., Neuberg, J. (Eds.), Volcano Instability on the Earth and other Planets. Geol. Soc. London, Spec. Pub., vol. 110, pp. 179–192.

Regione Siciliana-Assessorato LL.PP., 1994. Lavori di utilizzazione delle acque di Piedimonte Etneo per l'approvvigionamento idrico della città di Catania. Unpubl. technical report.

Rust, D., Neri, M., 1996. The boundaries of large scale collapse on the flanks of Mount Etna, Sicily. In: McGuire, W.J., Jones, A.P., Neuberg, J. (Eds.), Volcano Instability on the Earth and other Planets. Geol. Soc. London, Spec. Pub., vol. 110, pp. 169–177.

Rust, D., Behncke, B., Neri, M., Ciocanel, A., 2005. Nested zones of instability in the Mount Etna volcanic edifice, Italy. J. Volcanol. Geotherm. Res. 144, 137–153.

Tibaldi, A., Groppelli, G., 2002. Volcano-tectonic activity along structures of the unstable NE flank of Mt Etna (Italy) and their possible origin. J. Volcanol. Geotherm. Res. 115, 277–302.

van Wyk de Vries, B., Wooller, L.K., Cecchi, E., Murray, J.B., 2003. Spreading volcanoes: the importance of strike–slip faults. Geophys. Res. Abstr. 5 (abs. 02480).

Walter, T.R., Acocella, V., Neri, M., Amelung, F., 2005. Feedback processes between magmatic events and flank movement at Mount Etna (Italy) during the 2002–2003 eruption. J. Geophys. Res. 110 (B10), B10205. doi:10.1029/2005JB003688.

Wooler, L., van Wyk de Vries, B., Murray, J.B., Rymer, H., Meyer, S., 2004. Volcano spreading controlled by dipping substrata. Geology 32 (7), 573–576.